IEEE Access
Multidisciplinary | Rapid Review | Open Access Journal

Received August 8, 2019, accepted September 4, 2019, date of publication September 9, 2019,
date of current version September 30, 2019.

Digital Object Identifier 10.1109/ACCESS.2019.2940037

Damage Model Test of Prestressed T-Beam Under Explosion Load

HAN GUOZHEN, YAN BO, AND YANG ZAN
College of Aerospace Science and Engineering, National University of Defense Technology, Changsha 410072, China
Corresponding author: Yan Bo (boyan@nudt.edu.cn)

This work was supported by the National Natural Science Foundation of China under Grant 51708549.

ABSTRACT Bridge is an important infrastructure in road traffic, which may bear the accidental load of terrorist attacks and transportation accidents and explosions in its life cycle. In this paper, three groups of prestressed T-beam model tests were carried out in response to the terrorist explosion on the bridge deck. The results show that with the increase of explosive equivalent, the failure degree of prestressed steel reinforcement is aggravated, the number of anchorage falling off is increased, and the normal steel reinforcement evolved from failure to fracture. The fracture shape of the web of prestressed T-beam was "X", and the failure form on both sides of the web was roughly "工" shape. The number of concrete cracks increased, and the crack depth and the size of the crack increased. The local failure mode of T-beam evolved from seismic collapse to penetrating failure, and the residual bearing capacity of prestressed T-beam gradually decreased.

INDEX TERMS Contact blasting, damage mechanism, experimental research, PRC-T beam.

I. INTRODUCTION

As the throat of the transportation network, bridge plays a significant role in the national economy status and belongs to the third level of the five rings theory: infrastructure construction. This fully embodies the bridge of important military significance for the national security [1]. Because the large bridge structure usually locate in out-of-door places, the possibilities of terrorist attack and military strike are larger. Blast loadings produced by terrorist bombing or accidental gas explosion may cause significant structural damage, casualty and economic loss. Besides, the bridge structure damage is not easy to be repaired in time, which may cause greater loss to national economy and national security [2].

Due to the overall light dead weight and the advantages of prefabricated in the factory, the prestressed T beam (Prestressed Reinforced Concrete, PRC) is widely applied in the long-span bridge design. So the possibility of PRC-T beam bearing terrorist bombings and accidental explosion load is bigger. Because PRC-T beam belongs to the typical bridge target, conducting study about dynamic response of the blast loadings is practically valuable for engineering application.

Tianhua *et al.* [3] and Lujun *et al.* [4] respectively built different types of concrete beam scaling models and took the explosive equivalent, explosion location and explosion height as variables to analyze the concrete beam failure mode and damage mechanism under explosion load; Ming *et al.* [5], Qin *et al.* [6], Chen *et al.* [7] and other scholars respectively carried out research on explosion damage of single-piece reinforced concrete T-beam bridges with different sizes under different explosive conditions; The full-scale PRC-T beam bridge test carried out by Cofer *et al.* [8] was the single-plate PRC-T specimen. Besides, only the explosion location was analyzed as the influencing factor while the explosion equivalent was not studied in this test. Li *et al.* [9], Wang *et al.* [10], and Iqbal *et al.* [11]–[15] carried out related research on the blast resistance capacity of the reinforce concrete beams. Du [7], [17]–[22] focused on the dynamic of different types of T beam under the explosion to research the damage method and mechanism of various influence parameters such as the explosion equivalent, the explosion location and the beam size. Ishikawa *et al.* [23]–[25] studied the performance of prestressed concrete beams when subjected to impact loading. Bonded and unbonded prestressed beams were tested experimentally and analytically. It was found that, while static loading resulted in failure of the compression concrete for both the bonded and unbonded specimens, the higher load rate induced by impact resulted in the breaking of the prestressed tendon. Although the reinforced concrete T beam had been widely used since long time, however, the PRC- T

The associate editor coordinating the review of this manuscript and approving it for publication was Chandradip Patel.

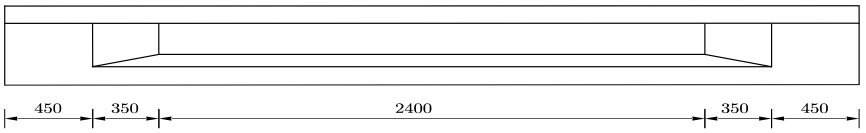

FIGURE 1. Side view of PRC-T beam model.

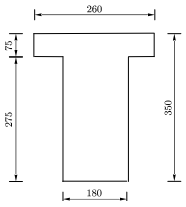

FIGURE 2. The cross section of beam-end.

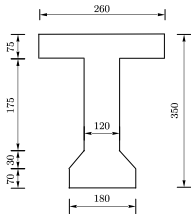

FIGURE 3. The cross section of mid-span.

beam just came into service in city bridge in recent years. Therefore, there is immature research about damage pattern and damage mechanism about PRC-T beam under explosion load at present.

At present, the research on dynamic response of PRC-T beam under explosion load is mainly focused on the numerical simulation, while the experimental studies in this filed is relatively few. In this paper, the model test of the explosion damage process of PRC-T beam was carried out to clarify the explosion damage mechanism of PRC-T beam, which can provide theoretical basis and data support for anti-explosion protection design and PRC-T beam blasting demolition.

II. MODEL TEST OVERVIEW

A. SAMPLE MODEL DESIGN

In order to further study the damage condition and failure mode of PRC-T beam under different explosion load, the PRC-T beam scaling model and test scheme were designed, while three groups of PRC-T beams specimens were cast with the same section properties and material properties, respectively named SJ-1, SJ-2, SJ-3. The test collected dynamic data such as steel bar strain and air overpressure during the PRC-T beam explosion failure process.

PRC-T beam model design was based on the ≪Road Bridge and Culvert Diagram≫ and ≪Highway Reinforced Concrete and Prestressed Concrete Bridge and Culvert Design Code≫ (JTG-D62-2004). The specimens were 4m in length, composed of upper flange, web and horseshoe structure. Besides, the specimens adopted variable section design. The model section size was shown in Fig.1-3, where Fig.1 shows the side view of PRC-T beam while Fig.2 shows the cross section of beam-end and Fig.3 shows the cross section of mid-span. According to the principle of static force similitude design, the structure was shrunk in the length, while the ratio of length was 0.13. And the reinforcement layout was designed by controlling the area reinforcement rate.

The rebar used in the PRC-T beam specimens mainly consisted of prestressed reinforcement, ordinary reinforcement

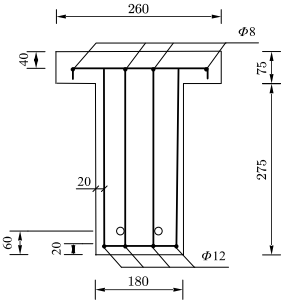

FIGURE 4. Beam-end reinforcement layout.

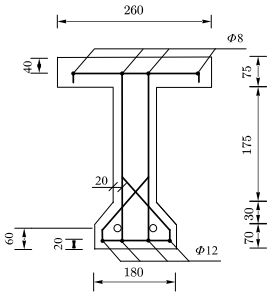

FIGURE 5. Mid-span reinforcement layout.

and anchorage bars, where the prestressed reinforcement was set as two bundles and each strand was equipped with a 15.2mm steel strand with tensile stress of 1860MPa. The prestressed tensioning method was the post-tensioning method and the tensioning control stress was $\sigma_{con} = 0.6f_{pk}$, while the tensile strength was 1860MPa. Ordinary rebar was HRB335 ribbed rebar with tensile strength of 280MPa and elastic modulus of 2.0×10^5 MPa. There were 4 longitudinal bars in the top flange plate, 2 constructional bars in the web and 4 tensile bars in the bottom horseshoe. The stirrup was reinforced. The reinforcement layout of all reinforcing bars meet the structural requirements. The transverse reinforcement layout meet the requirements of Section 5.7.2 and Section 9.4 of ≪Standard for Design of Highway Reinforced Concrete and Prestressed Concrete Bridges and Culverts≫. The beam-ends were compacted and arranged,

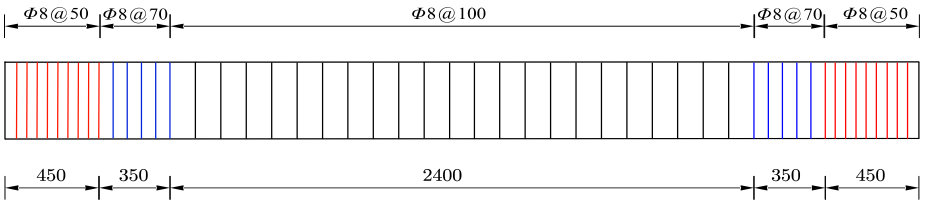

FIGURE 6. Stirrup reinforcement layout.

TABLE 1. Concrete material properties.

material	elasticity modulus MPa	Poisson's ratio	thermal coefficient of expansion m / $^{\circ}C$	volume weight KN/m^3	Standard compressive strength MPa	Standard tensile strength MPa
concrete	3.45E4	0.2	0.00001	25	32.4	2.64

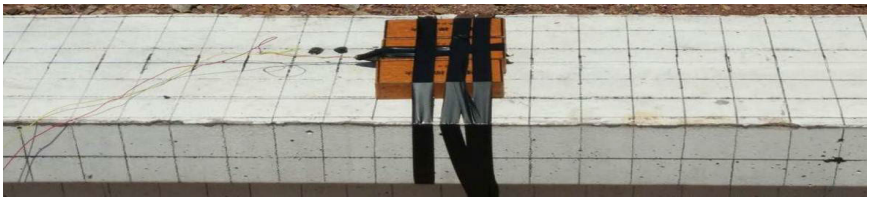

(a) SJ-1

(b) SJ-2

(c) SJ-3

FIGURE 7. Charge forms of three groups of PRC-T beams.

and the specific reinforcement is shown in Fig.4-6. And in the Fig.6, the red lines mean the distributed density of Φ8stirrup was 50mm; the blue lines mean the distributed density of Φ8stirrup was 70mm; the black lines mean the distributed density of Φ8stirrup was 100mm. C50 concrete was used in this test, and the material parameters are shown in Table 1.

B. TEST CONDITIONS

In this experiment, dynamic response and failure mode analysis of PRC-T beam were carried out by controlling explosive equivalent. The experimental design background was that the mid-span part of PRC-T beam bridge was subjected to terrorist explosion. The constraint condition of the specimens was simply supported constraint. The supporting point was

(a)SJ-1

(b)SJ-2

(c)SJ-3

FIGURE 8. The damage condition in mid-span.

(a) SJ-1 anchor

(b)SJ-2 anchor

(c) SJ-3 anchor

FIGURE 9. Anchorage falling off condition.

225mm high from the beam-end and the calculated span was 3.55m. The explosion mode was contact explosion, and the charge position was the surface of the top flange plate of the PRC-T beam mid-span. The explosion test was carried out in three groups, SJ-1, SJ-2 and SJ-3 respectively. There were the same shape, size, reinforcement layout and concrete strength, which can be considered to have the same mechanical properties. The TNT equivalent of SJ-1 beam, SJ-2 beam and SJ-3 beam were respectively 0.6kg, 1.0kg and 1.4kg, and the charging mode is shown in Fig.7.

III. TEST RESULTS AND ANALYSIS

A. REINFORCEMENT FAILURE OF PRC-T BEAMS AND ANALYSIS

1) PRESTRESS LOSS AND FAILURE ANALYSIS OF PRC-T BEAMS

Fig.8 shows the mid-span damage mode and failure of reinforcement of three specimens, which consist the bond between prestressed steel bars and concrete in the mid-span and the mid-span deflection. Fig.9 shows the different anchorage loss conditions at both ends of three PRC-T beams. The PRC-T beam specimen of different explosive equivalent produced different damage forms in the mid-span, where the concrete outside the PRC-T beam layoff and spall. As the explosive equivalent increased, the size of blasting crater and the depth of the crater in the mid-span gradually increased. The anchorage of SJ-1 specimen were both no-falling off; the prestressed tendon was detached from the concrete, while the bond state reduced substantially; besides, cracks appeared at the beam-end and in the mid-span, resulting in the reduction of the overall concrete strength and the subsequent loss of the prestress in the PRC-T beam. In the mid-span of SJ-2 specimen, the bottom horseshoe of the specimen showed deeply concrete stripping; there were only few part of the prestressed tendon and the concrete remaining bonded; and there was one of the two anchorages at the beam-end came into falling off. The anchorage at both end of SJ-3 specimen did not appear to be unanchored. It can be found from Fig.8(c) that the mid-span concrete was seriously collapsed and could not continue to bear any load. Therefore, it can be judged that these two strands of prestressed steel of SJ-3 specimen were completely failed.

Fig.10 shows the measurement diagram of the mid-span deflection of SJ-1 specimen. The measurement results showed that the initial height from the bottom of the beam is 36.5cm while the terminate height was 39.2cm relatively after the blast loading. There was an upward deflection

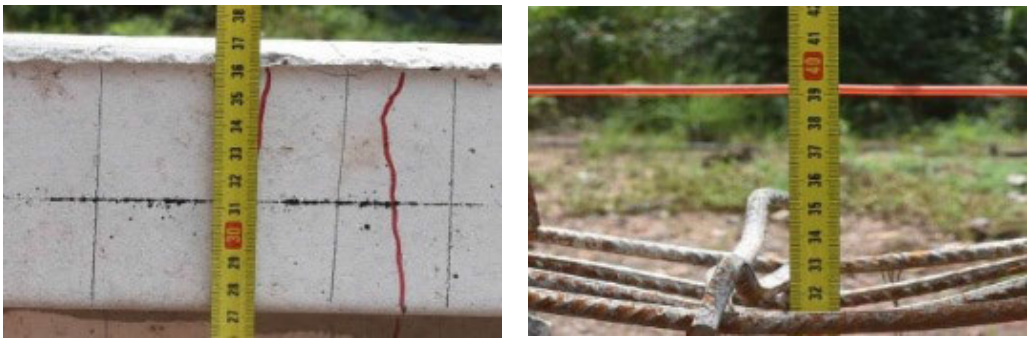

(a) The beam end deflection (b) the span center deflection

FIGURE 10. Deflection measurement results of SJ-1 beam.

TABLE 2. Failure statistics of prestressed rebar.

Beam number	Failure number of prestressed tendons	Number of prestressed tendon losses of beam	Beam end anchors
SJ-1	0	2	Neither anchorage failed to falling off
SJ-2	1	1	One prestressed rebar was still anchored but another prestressed bar was unanchored
SJ-3	2	0	Both unanchored

of 2.7cm, which did not meet the assumption of failure of prestressed reinforcement. Therefore, the prestressed reinforcement of SJ-1 under 0.6kg TNT was incomplete failure. The upward deflection of SJ-2 under 1.0kg TNT measured by the same method was 1.8cm, indicating that the anchorage was not falling off and the prestressed tendon had not completely failed. And there was serious collapse and no upward deflection of the SJ-3 under 1.4kg TNT. Failure statistics of prestressed bars of SJ-1 specimen, SJ-2 specimen and SJ-3 specimen are shown in table 2:

As shown in Table 2, with the increase of explosive equivalent, the failure risk of prestressed reinforcement increased gradually with the explosion load. There were two reasons for the failure of prestressed steel bars: the anchorage at the beam-end falling off and the concrete losing its bearing capacity, where the former failure occurred in the prestressed steel bars of SJ-2 specimen and the latter failure occurred in the two prestressed steel bars of SJ-3 specimen. As the cracks appeared on the concrete surface at the beam-end and in the mid-span, the strength of the concrete decreased and the no-failing prestressed bars also showed the loss of prestress. By contrastive analyzing of three groups of PRC-T beam on the anchorage falling off, the concrete stripping and the bonding state between concrete and prestressed reinforcement, the result showed that with the increasing of explosive equivalent, the cohesive condition of prestressed reinforcement and concrete was even worse, the external concrete of PRC-T beam loss more, the damaged condition in the mid-span gradually aggravated, upward deflection decreased. The SJ-3 specimen came into serious collapse and even the bottom horseshoe parts directly contacted with the ground. Besides, the quantity of the anchorage falling off and the prestressed reinforcement failure also gradually aggravated with the increasing of explosive equivalent. Above all, the explosive equivalent and PRC-T beam positively related to the failure of prestress and the damage condition.

2) FAILURE AND ANALYSIS OF ORDINARY REINFORCEMENT OF PRC-T BEAMS

The tensile stress of ordinary steel bar in PRC-T beam exceeded the elastic limit when subjected to explosion load, resulting in different degrees of plastic deformation. The failure patterns of ordinary steel bar in the three groups of specimens are shown in Fig.11. As that can be seen from Fig.11 (3), the 4 single longitudinal reinforcement in the top flange plate were peeled off from concrete. Besides, there were large deformation and destruction in the mid-span of SJ-1 specimen. Under 0.6 kg TNT explosion load, there were 4 longitudinal reinforcement in the top flange plate, 4 stirrup bars in the mid-span and 2 constructional reinforcement bars in the bottom horseshoe exposed to the air. And 4 longitudinal bars in the flange plate bent outward and downward, while 4 stirrup bars bent hook parts came into large deformation and 2 constructional reinforcement bars extruded from the concrete without obvious deformation; There were 4 longitudinal bars in the top flange plate, 5 stirrup in the mid-span and 2 constructional reinforcement bars in the web of the SJ-2 specimen under 1.0 kg TNT explosion load exposed to the air. And 4 longitudinal reinforcement bars in the flange plate bent larger deflection outward and downward, while one of the 4 longitudinal reinforcement bars, locating on the outer flange, produced too much deformation to escaping from the

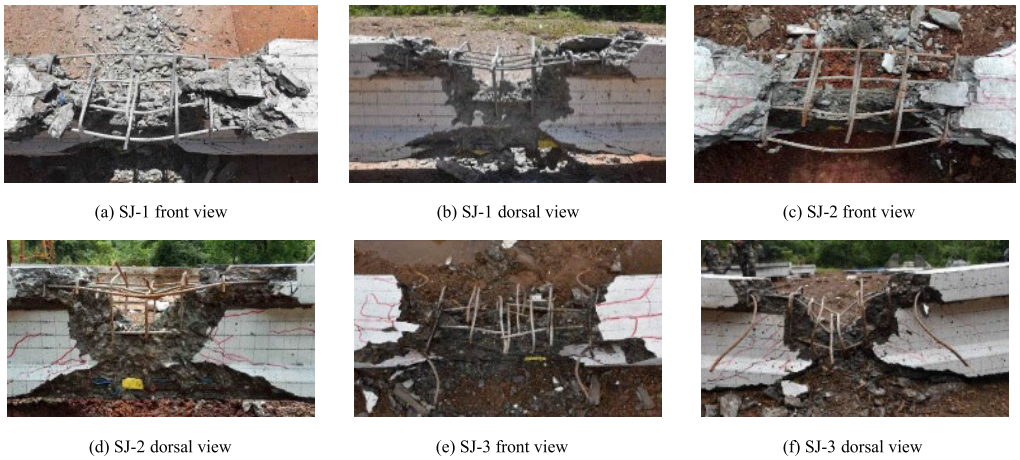

(a) SJ-1 front view (b) SJ-1 dorsal view (c) SJ-2 front view

(d) SJ-2 dorsal view (e) SJ-3 front view (f) SJ-3 dorsal view

FIGURE 11. Failure of ordinary steel bars of the specimens.

TABLE 3. The failure morphology statistics of the ordinary rebar damage.

Specimen number	The upper longitudinal bar	Stirrup	Waist muscle
SJ-1	Four deformation	4 deformation	2 had no obvious deformation
SJ-2	4 badly deformed	5 seriously deformed	2 had no obvious deformation
SJ-3	4 fracture	6 seriously deformed	2 had obvious deformation

stirrup lateral restraint. Besides, 5 stirrup bars formed serious deformation, where 3 of the 5 stirrup bars separated with longitudinal reinforcement in vertical separation. There were two constructional reinforcement bars occurring completely exposed but no obvious deformation; There were 4 longitudinal bars in the top flange plate, 6 stirrup in the mid-span and 2 constructional reinforcement bars in the middle web of the SJ-3 specimen under 1.4 kg TNT explosion load exposed to the air. Comparing to SJ-1 and SJ-2, the reinforcement damage of SJ-3 was the most obvious and serious. All of the four longitudinal reinforcement in the flange plate occurred fracture failure; There were 2 longitudinal reinforcement bars on the outer flange bending deformation backward and downward after fracture while 2 longitudinal reinforcement bars on the inner flange plate bending deformation outward and downward after fracture. 6 stirrup bars occurred serious deformation and the relative position of stirrup and longitudinal reinforcement were altered obviously. 2 constructional reinforcement bars completely were exposed to air and produced obvious downward bending deformation.

With the increase of explosive yield, the longitudinal reinforcement of the top flange plate ruptured first. Second, the stirrups in the mid-span of all the three specimens were fractured. Comparing the result of the three specimens, the amount of damaged steel bars was positively correlated with the explosive equivalent. Because the distance to the explosion center of the constructional reinforcement was large compared with longitudinal reinforcement and stirrup, only the deformation of constructional reinforcement of SJ-3 specimen was obvious. The failure morphology statistics of the ordinary rebar damage of SJ-1, SJ-2 and SJ-3 are shown in table 3.

Basing on the data of Table 3, the four longitudinal bars on the top flange plate of PRC-T beam were all destroyed under the three explosive equivalent. With the increase of explosive yield, the destruction of the longitudinal bars of the top flange plate was gradually transformed from deformation to fracture. The stirrups of the three PRC-T beam specimens were all ruptured, but more stirrups were destroyed with the increase of explosive equivalent. The constructional reinforcement was far away from the explosion center and the shock strength decreased with the increase of the distance to the explosion center. Therefore, only the deformation of the constructional reinforcement of SJ-3 specimen was obvious relatively.

B. PRC-T BEAM CONCRETE FAILURE MODE

1) CONCRETE BREAKAGE

The damage of concrete block manifested as the concrete flying away and peeling off from the explosion core to forming the crevasse and crater, which was roughly in the shape of ''X''. Concrete flying and flaking appeared on both the front and back of the PRC-T beam surfaces. With the increase of explosive equivalent, the crack depth at the web gradually increased, and the concrete damage condition of the specimen is shown in Fig.12 and 13. According to the failure modes of the three PRC-T beams, it can be concluded that the failure mode was roughly ''X'' shaped and there was also a funnel-shaped explosion pit, under the condition of contact

(a) SJ-1 upper flange front 1

(b) SJ-1 upper flange front 2

(c)SJ-1 anterior flank of web rupture

(d) SJ-1 posterior flank of web rupture

FIGURE 12. SJ-1 photos of concrete breakage.

explosion on the top of the mid-span flange plate. The failure forms on both sides of the PRC-T beam were roughly "工" shaped, and the remaining height of the web was inversely proportional to the explosive equivalent.

This paper statistically collected the length of lateral facture of upper flange, fracture length inside upper flange, length of median web rupture, height of crater in the mid-web, and length of upper horseshoe and length of lower horseshoe data. Based on these collected data, the PRC-T beam under the condition of contact explosion damage of concrete were analyzed. The detailed data about the damage of three groups of PRC-T beam are shown in Table 4.

According to the analysis in Table 4, it can be found that under the explosion load, the length of the outer of crevasse on the top flange plate and the breakage length of the lower horseshoe were larger, while the length of the inner of crevasse on the top flange plate, the crater length and height of the mid-web and the breakage length of the upper horseshoe were smaller. The length of the inner of the crevasse on the top flange plate, the crater length and height of the mid-web and the height of the funnel-shaped crater were related to the charge. And the different breakage size increased with the increase of the charge. By comparing the variation law of the fracture length under different explosive equivalent, it can be concluded that the response degree of the fracture length of the outer side of the upper flange and the horseshoe of the three PRC-T beams to the explosive yield were smaller because the detonation distance of the upper flange and the horseshoe to the explosion center were larger. The inner side of the upper flange and the web directly below the detonation center were greatly affected by the explosive yield. In other words, these two part suffering more serious damage.

2) CONCRETE CRACKS IN PRC-T BEAM

In order to further analyze the development of concrete cracks in PRC-T beam under contact explosion condition, the location and number of concrete cracks were recorded and counted in this paper. It can be seen from Fig. 14 and 15 that the crack of SJ-1 specimen was relatively complex but the crack distribution was approximately symmetrical on both sides of PRC-T beam. So the number of crack of the left half beam can be selected for analysis. The crack condition of the three PRC-T beams can be statistically analyzed. The crack distribution is shown in Table 5. This paper collected the crack number from the left beam end to the mid-span. Besides, four groups of data were collected with 0.5m as the unit length. And the distribution of crack of three specimens were shown in Fig.14-19.

The data in Table 5 shows that the cracks in the three specimens were mainly concentrated in the mid-span and the bearing position. Besides, most cracks of the mid-span were inclined cracks while the cracks near the bearing were mainly perpendicular to the axis direction. The number of cracks and damage degree at the bearing were significantly lower than those at the mid-span.

C. FAILURE MODE ANALYSIS OF PRC-T BEAM

1) ANALYSIS OF LOCAL FAILURE MODE

The explosive yield and thickness of concrete structures are closely related to the local failure mode. When the structure

(a) SJ-2 upper flange front1

(b) SJ-2 upper flange front 2

(c) SJ-2 anterior flank of web rupture

(d) SJ-2 Posterior flank of web rupture

(e) SJ-3 upper flange front 1

(f) SJ-3 upper flange front 2

(g) SJ-3 anterior flank of web rupture

(h) SJ-3 posterior flank of web rupture

FIGURE 13. **Photos of SJ-2, SJ-3 concrete breakage.**

TABLE 4. **Statistical table of specimen fracture size.**

Specimen number	Length of lateral tear of upper flange (cm)	Fracture length inside upper flange (cm)	Length of median web rupture (cm)	Height of crater in the mid-web (cm)	Length of upper horseshoe (cm)	Length of lower horseshoe (cm)
SJ-1	73	38	26	6	35	81
SJ-2	72	41	33	8	39	92
SJ-3	72	52	47	13	34	90

TABLE 5. Statistical table of crack number of specimens.

Specimen number	0-0.5m	0.5-1m	1-1.5m	1.5-2m
SJ-1	6	3	2	8
SJ-2	7	3	2	10
SJ-3	7	3	2	12

FIGURE 14. Left half span crack distribution of SJ-1.

FIGURE 15. Right half span crack distribution of SJ-1.

FIGURE 16. Left half span crack distribution of SJ-2.

FIGURE 17. Right half span crack distribution of SJ-2.

FIGURE 18. Left half span crack distribution of SJ-3.

was certainly thick, with the increase of explosive yield, there would be usually occurring three failure modes in sequence, which were namely impact failure, seismic collapse failure and penetrating failure. The outer side of the concrete of the upper flange of the three groups of specimens occurred cracks while longitudinal and stirrup came into fractures or serious deformation, indicating impact failure at the top of the PRC-T beam. The concrete of the horseshoe part was separated from the concrete, and deep oblique cracks appeared along the lower crevasse. Some bottom longitudinal bars and prestressed bars were separated from the concrete, meeting the failure conditions of seismic collapse. Funnel-shaped crater appeared on the top of the specimens and the web were loosened. At the bottom, the concrete was stripped off, and the web formed "X" shaped crevasse on the facade. The impact funnel-shaped crater of SJ-1 and SJ-2 and the corresponding seismic collapse funnel-shaped crater were penetrating. Besides, the degree of damage was between the seismic collapse and penetrating failure, which was defined as serious seismic collapse. The impact funnel-shaped crater and seismic collapse funnel-shaped crater of SJ-3 completely run through, which belonged to the local failure in the form of penetrating failure. It can be concluded from the failure modes of the three specimens that with the increase of the charge, the size of the "X" shaped fracture of the upper flange gradually increased; the cracks near the fracture area gradually increased; the top longitudinal and stirrup gradually transformed from deformation to fracture; the crater depth in the funnel-shaped crater and the number of diagonal cracks on the web and the peeling thickness of the concrete at the horseshoe also increased gradually.

2) OVERALL FAILURE MODE ANALYSIS

There are three situations in which the whole structure was destroyed under the explosion load. The first is the whole structure destroyed by the non-contact blast air shock wave; the second is the whole structure destroyed by the local

FIGURE 19. Right half span crack distribution of SJ-3.

FIGURE 20. Mid-span transverse fracture of SJ-1.

FIGURE 21. Mid-span vertical fracture of SJ-1.

contact explosion under the initial stress, and the third is the two situations mentioned above at the same time. The specimens in this paper belongs to the second type of integral failure.

Referring to the method proposed by Mengshen *et al.* [26], [27] to calculate the residual flexural capacity of the section to study the overall failure mode of the specimens. Combining with the test data of three PRC-T beams, the ratio of the residual bearing capacity was defined as the damage coefficient to analyze the overall failure mode of the three PRC-T beams. The specific method was as the following: the damage coefficient $R = 1-M/M_0$ is defined, where M is the flexural bearing capacity of the specimen after failure, and M_0 is the initial flexural bearing capacity of the specimen before failure. When $0 < R < 0.25$, the specimen did not occur overall failure. When $0.25 < R < 0.5$, the specimen suffered slight overall damage. When $0.5 < R < 0.75$, serious overall failure occurred. When $0.75 < R < 1$, severe overall damage occurred to the specimen.

Firstly, the height of the compression zone is x = 10cm $> h'_f = 8cm$, indicating that the specimen belongs to the T beam of the second section. According to the calculation method of the initial flexural capacity of the T-beam with the second section, the initial flexural capacity of the three PRC-T beams before the test was calculated. The actual height of the compression zone x was calculated according to the formula below

$$\Sigma x = 0 \quad f_c(b'_f - b)h'_f + f_c bx = f_y A_s + f_p A_p \tag{1}$$

where, b is the width of the horseshoe part, evaluating b=0.12m in this paper, and x=13cm calculated by formula (1). In accordance with equation (2), the moment of the prestressed steel bar was calculated based on the torque balance

$$\Sigma M = 0 \quad M_r = f_c(b'_f - b)h'_f(h_0 - \frac{h'_f}{2}) + f_c bx(h_0 - \frac{x}{2}) \tag{2}$$

where, h_0 is the effective height of the section, and 0.32m was taken to obtain $M_{r0} = 174.7\text{kN} \cdot \text{m}$. The residual moment bearing capacity of the specimen after damage was controlled by the equivalent section of mid-span concrete. In other words, when the critical height of the equivalent section of mid-span concrete reached the designed strength of concrete, the specimen would reach the critical moment bearing capacity state. At this point, the bending moment bearing capacity is:

$$M_{r1} = f_c b_1 x_1 (h_{01} - \frac{x_1}{2}) \tag{3}$$

In code for design of concrete structures (GB50010-2010), the height of compression zone of C50 concrete suitable for reinforced PRC-T beams was specified as $x \leq \xi_b h_0$, where ξ_b was 0.4; at the end of the test, the mid-span section was in the state of overbar, which caused the neutral surface moved down and the height of the compression zone increased. According to the mathematical expression of equation (3), when $x=h_0$ and $\xi = 1$, the calculation result of section bending capacity was the maximum value. In the calculation process, the height of the compression zone was taken $\xi = 1$ conservatively, that means the height of compression zone was $x_1 = h_{01}$. The remaining bearing capacity was calculated $22.46kN \cdot m$ from equation (3), which was only 12.8% of the initial bearing capacity. The bending moment of the PRC-T beam was $2.42kN \cdot m$ in the mid-span under dead weight. Then after the test, the bending capacity of SJ-1 could resist 9.26 times dead weight by calculated. Since the equivalent section taken into account the looseness and reduction of concrete, the strength reduction caused by concrete damage was not considered repeatedly in the calculation of section flexural bearing capacity. The bending capacity of SJ-2 specimen was also calculated according to equation (3), which was only 7% of the initial bearing capacity. After the test, the bending capacity of SJ-2 specimen could resist 5.02 times of its own dead weight. After the test of SJ-3 specimen, the mid-span section completely failed and the specimen lost its stability

TABLE 6. Analysis table of overall failure model.

Specimen number	Loading situation	M_{r0}(kN·m)	M_r(kN·m)	M_r/M_{r0}(%)	R	Damage level
SJ-1	0.6kgTNT		22.46	12.8	0.872	Serious damage
SJ-2	1.0kgTNT	174.7	12.14	7	0.93	Serious damage
SJ-3	1.4kgTNT		0	0	1	Serious damage

FIGURE 22. Mid-span transverse fracture of SJ-2.

FIGURE 23. Mid-span vertical fracture of SJ-2.

and collapsed to the ground. Besides, the mid-span section concrete completely lost its bearing capacity, and the two prestressed rebar both relaxed and failed. According to the calculation formula of flexural capacity: $M_{r3} = f_c b_3 x_3 (h_{03} - x_3/2)$, $f_c = 0$ after concrete loses compression capacity, then $M_r = 0$.

Fig.20 and 21 show the mid-span fracture of SJ-1, while Fig.22 and 23 show the mid-span fracture of SJ-2.These pictures give the transverse and vertical mid-span fracture.

Table 6 is a comparative analysis table of the overall failure modes of the three specimens.

It can be seen from Table 6 that the flexural capacity damage coefficients of the normal section were 0.872, 0.93 and 1 respectively after the contact explosion of the three PRC-T beam specimens, all of which were serious overall damages. Besides, the damage coefficient of flexural capacity of normal section increased with the increase of explosive yield.

IV. CONCLUSION

In this paper, the model test was carried out to investigate the research hotspot about the terrorist explosion load on PRC-T beam. Basing on the result, it can be analyzed that the relation between the PRC-T beam failure mode and mechanism of explosive damage and the explosive equivalent. The main research results, conclusions and suggestion about T beam design are as follows:

(1) Under contact explosion load, the failure pattern at the top of the PRC-T beam was roughly "X" shaped and there was occurring also the funnel-shaped explosion crater; the failure form on both sides of PRC-T beam were roughly "工" shaped. Prestress loss or failure, longitudinal reinforcement and stirrup, etc. The cracks were distributed symmetrically, most of which were inclined cracks in the mid-span and were perpendicular to the axis of the support.

(2) By comparing and analyzing the failure forms of concrete, the development of concrete cracks and the failure of steel bars under different explosive yields, it can be concluded that with the increase of explosive yields, the damage degree of steel bars increased, the number of concrete cracks increased, and the crack depth and the size of concrete breakage gradually increased;

(3) Combined with the fracture size and crater shape of PRC-T beam under different explosive yields, it can be concluded that with the increase of explosive yield, the local failure mode of PRC-T beam evolved from seismic collapse to penetrating failure;

(4) The residual bearing capacity of three groups of PRC-T beams was calculated, and combined with the macroscopic failure phenomenon of PRC-T beams, it was obtained that with the increase of explosive equivalent, the residual bearing capacity of PRC-T beams gradually decreased while the damage degree gradually increased.

(5) The PRC-T beam should be deigned with strengthening the mid-web, especially the joint part of flange plate and web, in order to induce the damage caused by stress concentration. In actual construction, it's better to thicken web properly and strengthening the joint with steel plate of good stiffness.

ACKNOWLEDGMENT

The author gratefully acknowledge Lecturer Liu Fei for his valuable suggestions and guidance on the design, implementation and data collection of the experiment, especially thanks to his guidance for the analysis of damage phenomenon and failure model and mechanism. And graduate students

Li Baoyan and Yang Zan for their great contributions to the experiment.

REFERENCES

[1] Y. Chunyan and G. Xuaneng, "Research on anti-explosion design methods of building structures," *Fujian Archit. Construct.*, vol. 7, pp. 59–60, 2010.

[2] Z. Xinming, J. Zhigang, and B. Zhihai, "Characteristics of traffic terrorist attacks and research on anti-terrorism measures," *Traffic Eng. Technol. Nat. Defence*, vol. 1, pp. 4–7 and 31, 2011.

[3] J. Tianhua, Y. Yunfeng, and G. Jie, "Damage analysis of concrete t-beam under explosion," *World Building Mater.*, vol. 6, pp. 36–39, 2015.

[4] C. Lujun, D. Gang, and G. Qin, "Test of concrete t-beam bridge under blasting impact load," *Eng. Blasting*, vol. 1, pp. 8–12 and 19, 2018.

[5] Y. Ming, L. Yuan, and H. Siwei, "Experimental study on stiffness modification of effective prestress of concrete t-beam," *J. China Foreign Highway*, vol. 1, pp. 68–72, 2015.

[6] F. Qin, L. Jinchun, and Z. Yadong, "Finite element analysis of failure modes of reinforced concrete beams under blast load," *Eng. Mech.*, vol. 2, pp. 1–8, 2001.

[7] W. Chen, H. Hao, and S. Chen, "Numerical analysis of prestressed reinforced concrete beam subjected to blast loading," *Mater. Des.*, vol. 65, pp. 662–674, Jan. 2015.

[8] W. F. Cofer, D. S. Matthews, and D. Mclean, "Effects of blast loading on prestressed girder bridges," *Shock Vib.*, vol. 19, no. 3, pp. 1–18, 2015.

[9] M.-S. Li, J. Li, H. Li, C.-C. Shi, and N. Zhang, "Deformation and failure of reinforced concrete beams under blast load," *Explosion Shock Waves*, vol. 35, no. 3, pp. 177–183, 2015.

[10] W. Wei, L. Ruichao, W. Biao, L. Lin, H. Jiarong, and W. Xing, "Research on damage criteria of reinforced concrete beams under blast load," *Acta Armamentarii*, vol. 8, pp. 1421–1429, 2016.

[11] M. A. Iqbal, A. Rajput, and N. K. Gupta, "Performance of pretressed concrete targets against projectile impact," *Int. J. Impact Eng.*, vol. 110 pp. 15–25, Dec. 2017.

[12] Y. Shi, Z.-X. Li, and H. Hao, "A new method for progressive collapse analysis of RC frames under blast loading," *Eng. Struct.*, vol. 32, no. 6, pp. 1691–1703, 2010.

[13] Y. Sieffert, G. Michel, P. Ramondenc, and J.-F. Jullien, "Effects of the diaphragm at midspan on static and dynamic behaviour of composite railway bridge: A case study," *Eng. Struct.*, vol. 28, no. 11, pp. 1513–1524, 2006.

[14] Y.-Z. Li, X.-J. Wang, X.-H. Guo, H. Cao, and K. Zhao, "Experimental study on anti-impact properties of a partially prestressed concrete beam," *Explosion Shock Waves*, vol. 26, no. 3, pp. 256–261, May 2006.

[15] Q. Fang, M.-L. Du, and L. hen, "Blast-resistant properties of beams consisting of nonlinear elastic large deformation materials," *Explosion Shock Waves*, vol. 29, no. 1, pp. 7–12, 2009.

[16] L. Zhongxian, S. Yanchao, S. Xiangsheng, "Failure assessment method of reinforced concrete slab under blast load," *J. Building Struct.*, vol. 30, no. 3, pp. 60–66, 2009.

[17] D. Gang, *Dynamic Response of Reinforced Concrete T Beam Bridge and Box Girder Bridge Under Explosion Load*. Wuhan, China: Wuhan Univ. of Science and Technology, 2018.

[18] J. Tianhua, Y. Yunfeng, G. Jie, and C. Lujun, "Damage analysis of concrete T beam under explosion," *Building Mater. World*, vol. 36, no. 3, 2015.

[19] J. Tianhua, Y. Yunfeng, and G. Jie, "Damage analysis of concrete t-beam under explosion," *World Building Mater.*, vol. 6, pp. 36–39, 2015.

[20] M. Lee and H.-G. Kwak, "Blast and impact analyses of RC beams considering bond-slip effect and loading history of constituent materials," *Int. J. Concrete Struct. Mater.*, vol. 12, p. 32, Dec. 2018.

[21] G. Xiang, L. Dong, and C. Lu, "Study on the damage of simple t-beam under explosion impact," *J. Qingdao Univ. Technol.*, vol. 37, no. 3, pp. 26–31, 2016.

[22] D. Xiaoye, *Research on Performance and Flexural Capacity of Highway Prestressed Concrete T Beams*. Shijiazhuang, China: Shijiazhuang Railway Univ., 2016.

[23] N. Ishikawa, H. Enrin, S. Katsuki, and T. Ohta, "Dynamic behavior of prestressed concrete beams under rapid speed loading," in *Structures Under Shock and Impact*. Billerica, MA, USA: Computational Mechanics, 1998, pp. 717–726.

[24] N. Ishikawa, S. Katsuki, and K. Takemoto, "Dynamic analysis of prestressed concrete beams under impact and high speed loadings," in *Structures Under Shock and Impact*. Billerica, MA, USA: Computational Mechanics, 2000, pp. 247–256.

[25] N. Ishikawa, S. Katsuki, and K. Takemoto, "Incremental impact test and simulation of prestressed concrete beam," in *Structures Under Shock and Impact*. Billerica, MA, USA: Computational Mechanics, 2002, pp. 489–498.

[26] L. Mengshen, L. Jie, and L. Hong, "Deformation and failure of reinforced concrete beams under explosion load," *Explosion Shock Waves*, vol. 2, pp. 177–183, 2015.

[27] P. Sheng, *Dynamic Response Analysis of Concrete T-Beam Bridge Under Blast Load*. Wuhan, China: Wuhan Univ. Science Technology, 2016.

HAN GUOZHEN received the bachelor's degree from the National Defense University of Science and Technology, in 2017, where he is currently pursuing the master's degree. His current research interests include structural design, mechanical analysis, and anti-explosion dynamic response of prestressed T-beam bridges, with emphasis on the dynamics research of bridges at home and abroad.

YAN BO is currently a Professor, carrying out research, with the Department of Applied Mechanics, College of Aerospace Science and Technology, National University of Defense Technology. He has published more than ten SCI and EI journal articles. His current research interests include dynamic analysis of bridge structure, application of finite-element method in mechanical analysis, and theoretical research of structural mechanics.

YANG ZAN received the bachelor's degree from the National University of Defense Technology, in 2017, where he is currently pursuing the master's degree. His current research interests include structural design and mechanical analysis and dynamic response research of prestressed box girder bridges, with emphasis on the dynamics research of bridges at home and abroad.